

ON THE INTERNAL REPRESENTATIONS OF GRAPH METANETWORKS

Taesun Yeom & Jaeho Lee

Pohang University of Science and Technology (POSTECH)
 {tsyeom, jaeho.lee}@postech.ac.kr

ABSTRACT

Weight space learning is an emerging paradigm in the deep learning community. The primary goal of weight space learning is to extract informative features from a set of parameters using specially designed neural networks, often referred to as *metanetworks*. However, it remains unclear how these metanetworks learn solely from parameters. To address this, we take the first step toward understanding *representations* of metanetworks, specifically graph metanetworks (GMNs), which achieve state-of-the-art results in this field, using centered kernel alignment (CKA). Through various experiments, we reveal that GMNs and general neural networks (*e.g.*, multi-layer perceptrons (MLPs) and convolutional neural networks (CNNs)) differ in terms of their representation space.

1 INTRODUCTION

The field of weight space learning has gained a lot of attention these days. Inspired by the concept of “geometric deep learning” (Bronstein et al., 2021), recent works have tended to focus on designing architectures that incorporate the symmetries underlying the parameter space of neural networks (NNs) (*e.g.*, permutation, scaling, etc.) (Navon et al., 2023; Zhou et al., 2023). These architectures are generally referred to as *metanetworks*. Building on these seminal works, graph metanetworks (GMNs)—which process the parameters of neural networks as a graph structure—not only demonstrate superior performance across various tasks but also offer practical ease of use, as they can handle heterogeneous architectures and naturally accommodate permutation symmetry in the parameter space without the need for laborious equivariant layer design (Lim et al., 2024; Kofinas et al., 2024).

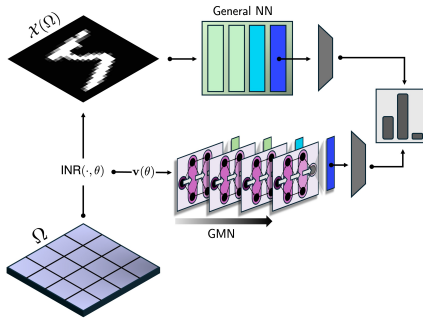


Figure 1. GMN vs. General NN.

Despite recent advances in this field, state-of-the-art metanetworks (*e.g.*, ScaleGMN (Kalogeropoulos et al., 2024)) have been observed to perform well on certain tasks (*e.g.*, classifying MNIST INRs) but poorly on others (*e.g.*, classifying CIFAR-10 INRs). This discrepancy naturally raises a question: *what do these types of networks really learn solely from the parameters of NNs?* Hence, in this work, we empirically investigate “what GMNs learn” through the lens of *representations* (*i.e.*, hidden features), which provide powerful insights for understanding NNs.

Contributions. Our main goal is to understand the representations in GMNs. To this end, we focus on an INR classification task for GMNs and, in turn, compare the representations they learn with those of MLPs and CNNs (which we refer to as “general NNs”) performing standard image classification task (Fig. 1). We begin by examining the effect of random initialization on representations in both cases and find that it leads to randomness in representations in GMNs, but not in general NNs. Next, we analyze the similarity of representations across different architectures and reveal that the representations of GMNs differ from those of general NNs through the cross-architecture CKA. Lastly, we find that this difference in representations indeed affects prediction tendencies, suggesting that weight space learning may play a complementary role in representation learning.

2 PRELIMINARIES

In this section, we provide a brief overview of the similarity measure used in our work—centered kernel alignment (CKA)—along with a formal description of our setup. We note that the discussion of related work is provided in Appendix A, and more details in Appendix B.

Centered kernel alignment (CKA). CKA (Gretton et al., 2005) is a nonparametric similarity measure that is invariant to orthogonal transformations and isotropic scaling. Let $X \in \mathbb{R}^{n \times d_x}$ and $Y \in \mathbb{R}^{n \times d_y}$ the representations of NNs, and \mathbf{X} and \mathbf{Y} the corresponding kernel matrices (e.g., $\mathbf{X}_{ij} = K(X, X)_{ij}$). In our work, we consider the kernel function $K(\cdot, \cdot)$ to be linear (i.e., $\mathbf{X} = XX^\top$). Now, CKA is defined as

$$\text{CKA}(X, Y) = \frac{H(\mathbf{X}, \mathbf{Y})}{\sqrt{H(\mathbf{X}, \mathbf{X})H(\mathbf{Y}, \mathbf{Y})}}, \quad \text{where} \quad H(\mathbf{X}, \mathbf{Y}) = \frac{1}{(n-1)^2} \text{tr}(\mathbf{X}C\mathbf{Y}C). \quad (1)$$

In Eq. (1), $H(\cdot, \cdot)$ denotes the empirical estimator of Hilbert-Schmidt independence criterion (HSIC), and C is a centering matrix (i.e., $C = I_n - \frac{1}{n}\mathbf{1}\mathbf{1}^\top$). CKA is widely used in deep learning, specifically as a similarity measure for representations across different initializations (Kornblith et al., 2019), architectures (Raghu et al., 2021), and data modalities (Maniparambil et al., 2024).

GMNs vs. general NNs. As mentioned in the previous section, we compare GMNs with “general NNs” (specifically, MLPs and CNNs in our case). The difference between GMNs and general NNs is straightforward: the latter directly take “general data” as input, whereas GMNs take only parameters as input. Formally, we consider a signal $\mathbf{x} \in \mathcal{X}(\Omega)$ that lies in a domain Ω , and define ‘the function of an INR’ as $\text{INR}(u, \theta) : \Omega \rightarrow \mathcal{X}(\Omega)$, where u is a set of discrete coordinates in Ω , and θ is parameters of INR. While general NNs process \mathbf{x} directly, GMNs process graph $\mathbf{v}(\theta) = (\mathcal{V}, \mathcal{E})$, referred to as *neural graph*. Note that $\mathbf{v}(\cdot)$ is a function that converts θ into a (directed acyclic) graph.

Our setup. In this work, we consider a supervised classification task with three different datasets: MNIST, Fashion-MNIST, and CIFAR-10. Precisely, for each dataset containing N data, we use $D_{\text{NN}} = (\mathbf{x}_n, y_n)_{n=1}^N$ for general NNs and $D_{\text{GMN}} = (\mathbf{v}(\theta_n), y_n)_{n=1}^N$ for GMNs. Here, \mathbf{x}_n and $\mathbf{v}(\theta_n)$ serve as input for general NNs and GMNs each, and $y_n \in \mathbb{R}^k$ is the corresponding label vector with k different classes. Note that θ_n represents the parameters of $\text{INR}_n(u_n, \theta_n)$, where the INR is trained to reconstruct \mathbf{x}_n . For GMNs, we perform an INR classification task where the GMN takes only $\mathbf{v}(\theta_n)$ as input to predict the label y_n . In contrast, general NNs learn to predict labels y_n directly from the input image \mathbf{x}_n . Additionally, we implement INRs using ‘sinusoidal representation networks’ (SIREN) architecture (Sitzmann et al., 2020), which employs a sine activation function. For GMNs, we adopt ScaleGMN (Kalogeropoulos et al., 2024) architecture.

3 ON THE INTERNAL REPRESENTATIONS OF GMNS: AN EMPIRICAL STUDY

In this section, we begin our investigation by analyzing the impact of initialization on representations. Next, to gain deeper insights, we compare the representations of GMNs with those of general NNs. Lastly, we examine how representations influence predictions. Before proceeding, we introduce important details relevant to this section.

- For all experiments in this section, we use four hidden layers for general NNs and four MP steps for GMNs. Moreover, when comparing CKA between ‘different architectures,’ we train general NNs until they achieve the highest test accuracy attained by GMNs for each dataset, since general neural networks always outperform GMNs when there are no constraints in the classification task.
- To calculate CKA, we use the activation matrix obtained from the test dataset at the k -th hidden layer in general NNs, and the features of the output node(s) (e.g., gray node in Fig. 1) after k MP steps in GMNs, both of which we set to have the same dimensions for per task. Here, we set $k \in \{3, 4\}$ due to the learning strategy of GMNs¹.

¹Since we consider a three-layer INR, we need at least three forward MP steps to propagate information from the input node to the output nodes. That is, for GMNs to “learn representations of the whole graph,” they require at least three update steps.

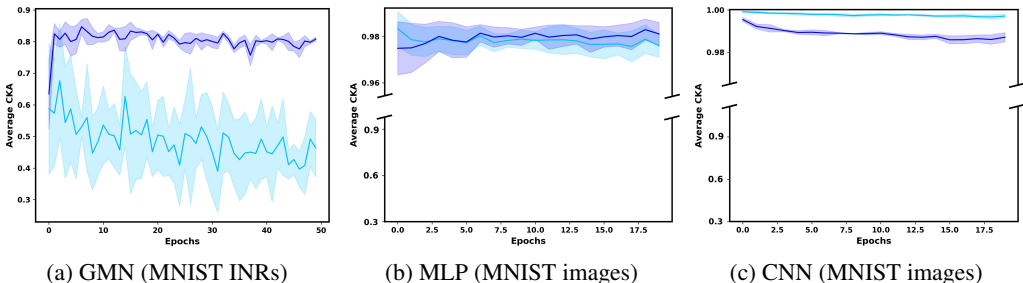


Figure 2. **Averaged CKA over five pairs of random GMNs, MLPs, and CNNs in MNIST classification.** The skyblue plot represents the averaged $\overline{\text{CKA}}(3, \mathbf{a})$, while the blue plot represents the averaged $\overline{\text{CKA}}(4, \mathbf{a})$ for each architecture.

3.1 ON THE IMPACT OF RANDOM INITIALIZATION

It is known that random initialization plays a crucial role in representations of NNs from various perspectives (see Appendix A). Building on this, we first study how random initialization in NNs affects their representations. We trained ten NNs with different initializations for each architecture and paired them within the same architecture, forming five pairs. For every training epoch, we compute the CKA for each pair using the test dataset and take the average per architecture, which we denote as $\overline{\text{CKA}}(k, \mathbf{a})$ for brevity.

In Fig. 2, we plot the dynamics of $\overline{\text{CKA}}$ throughout training. Observing the results for MLP and CNN cases, we see that random initialization does not significantly impact the representation similarity of general NNs, as indicated by consistently high CKA values (*i.e.*, between 0.9 and 1), regardless of the layer index. However, in the case of GMNs (Fig. 2a), $\overline{\text{CKA}}(3, \text{GMN})$ is significantly lower during training compared to general NNs. This may be due to the presence of projection layers in GMNs, which project node and edge features (which are originally scalar values) to a higher dimension using multi-layer linear networks. The intriguing part is that the representations do not converge (or at least do not increase) with each other throughout training. This indicates that “different initializations lead to different hidden representations in GMNs throughout training,” which may substantially affect the representations of the last step of MP. For instance, $\overline{\text{CKA}}(4, \text{GMN})$ are considerably lower than those of MLPs and CNNs (*i.e.*, almost 1) throughout training. Note that lower CKA does not reflect higher variance in classification accuracy (Table 2 in the Appendix).

Takeaways. Unlike general NNs, the effect of random initialization in GMNs is significant: it reduces the similarity of representations. In other words, random GMNs captures different representations depending on initialization.

3.2 GMNs AND GENERAL NNs LEARN DIFFERENT REPRESENTATIONS

Next, we conduct experiments to compare representations across architectures. Since the learning curve of test accuracy varies depending on both architecture and dataset, we compare representations only at the final epoch for a fair comparison. Additionally, we analyze the representations just before the linear classifier (*i.e.*, $k = 4$). Similar to the previous subsection, we compare five pairs within each group. However, in this case, we consider three different groups: GMN vs. MLP, GMN vs. CNN, and MLP vs. CNN. Here, we denote $\overline{\text{CKA}}(k, \mathbf{a} \leftrightarrow \mathbf{b})$ as the averaged CKA between two types of networks, \mathbf{a} and \mathbf{b} .

		Dataset		
		MNIST	Fashion-MNIST	CIFAR-10
CKA	GMN \leftrightarrow MLP	0.42 \pm 0.04	0.42 \pm 0.03	0.38 \pm 0.06
	GMN \leftrightarrow CNN	0.43 \pm 0.03	0.49 \pm 0.02	0.43 \pm 0.05
	MLP \leftrightarrow CNN	0.94 \pm 0.01	0.95 \pm 0.01	0.94 \pm 0.01
NHD	Random GMNs	0.041 \pm 0.002	0.137 \pm 0.006	0.229 \pm 0.007
	Random MLPs	0.022 \pm 0.001	0.045 \pm 0.007	0.062 \pm 0.009
	Random CNNs	0.023 \pm 0.002	0.036 \pm 0.002	0.062 \pm 0.004
	GMN \leftrightarrow MLP	0.050 \pm 0.002	0.192 \pm 0.007	0.349 \pm 0.013
	GMN \leftrightarrow CNN	0.058 \pm 0.002	0.175 \pm 0.006	0.350 \pm 0.013
	MLP \leftrightarrow CNN	0.033 \pm 0.001	0.093 \pm 0.004	0.145 \pm 0.009

Table 1. **Averaged CKA between different architectures and NHD from various cases.**

In Table 1 (CKA), we report $\overline{\text{CKA}}(4, \mathbf{a} \leftrightarrow \mathbf{b})$ along with its standard deviation, computed within each group. Interestingly, despite the three different network types achieving nearly the same test accuracy with the same classifier structure, the CKA value heavily depends on the combination of

architectures. For example, when comparing representations in general NNs (*i.e.*, MLPs vs. CNNs), the CKA value remains consistently high across various datasets. However, when comparing architectures from different groups (*i.e.*, GMNs vs. {MLPs, CNNs}), the CKA value is considerably lower than in the former case.

It is notable that, despite MLPs and CNNs being known to have different inductive biases, their final representations are still somewhat aligned. On the contrary, GMNs behave differently from general NNs, even though their test accuracies are almost identical to those of general NNs (see Table 2). These results suggest that the representations of GMNs and general NNs differ, *i.e.*, the representations learned from parameters and images are different.

Takeaways. By examining CKAs between GMNs and general NNs, we can see that GMNs learn representations differently from general NNs, whereas CNNs and MLPs learn in a similar manner.

3.3 ON THE PREDICTION TENDENCY OF GMNS

A natural question arises here: if GMNs and general NNs learn different representations, how do they achieve almost same test accuracies? While it is possible for different feature spaces to yield the same classification results, it is important to examine this from the perspective of predictions—specifically, whether the predictions made by GMNs are genuinely similar or different to those of general NNs.

To this end, we evaluate the normalized Hamming distance (NHD) (Hamming, 1950), which quantifies the difference between two sequences that consist of binary elements: each element in the sequence is defined as ‘1’ (if the prediction is correct) or ‘0’ (if it is not)². We report the averaged NHDs in Table 1, which are obtained by averaging the NHDs over five pairs for each case. First, we analyze the impact of random initialization on predictions (denoted as “Random networks”). In this case, GMNs exhibit a considerably higher NHD than general NNs, meaning that the predictions of GMNs are more variable. Furthermore, we evaluate the NHD across different architectures (denoted as “ $\mathbf{a} \leftrightarrow \mathbf{b}$ ”). It can be seen that the NHDs between MLPs and CNNs are low, whereas those between GMNs and general NNs are relatively high. This result indicates that the predictions made by GMNs and general NNs indeed differ, while MLPs and CNNs yield nearly identical predictions.

For an in-depth analysis, we investigate whether there are instances in which GMNs make correct predictions while general NNs fail in MNIST classification. We examine this in both our original setting—where general NNs achieve nearly the same test accuracy as GMN—and an additional setting in which general NNs are trained longer to reach better test accuracy (details are in Table 2). Surprisingly, in both cases, there exist instances that which GMN consistently makes correct predictions, whereas MLP and CNN fail across all cases (*e.g.*, Fig. 4), even if the lower test accuracy. This phenomenon implies that the representations of GMNs learned from “parameters” may complement the representations of general NNs learned from “visual signals.”

Takeaways. The different internal representations of GMNs and general NNs indeed impact predictions. Moreover, in some cases, there are samples that only GMNs can correctly classify.

4 CONCLUSIONS

In this work, we empirically investigate the representations of GMNs using CKA, comparing them to general NNs, specifically MLPs and CNNs. We find that random initialization has a significantly greater impact on the representations of GMNs than on those of general NNs. Furthermore, while general NNs tend to learn similar features, GMNs exhibit distinct representations, suggesting that they tend to capture different types of information depending on initialization. Finally, these differences in representation ultimately lead to differences in predictions.

Limitations and future directions. We focus on only one task of weight space learning (*i.e.*, INR classification), where the task does not reflect equivariance. Another limitation lies in our selection of general NNs, which we exclude widely used models, such as vision transformer (Dosovitskiy et al., 2021). However, we strongly believe that our work will inspire promising future directions for improving the performance of metanetworks, as well as other applications of them.

²NHD is computed as $d_H(p, q) = \frac{1}{N} \sum_{i=1}^N \mathbb{1}_{q_i \neq p_i}$, where $p = (a_1, \dots, a_N)$ and $q = (b_1, \dots, b_N)$ are the two sequences of networks’ predictions being compared, and N is the length of the test dataset.

REFERENCES

- Michael M Bronstein, Joan Bruna, Taco Cohen, and Petar Veličković. Geometric deep learning: Grids, groups, graphs, geodesics, and gauges. *arXiv preprint arXiv:2104.13478*, 2021.
- Alexey Dosovitskiy, Lucas Beyer, Alexander Kolesnikov, Dirk Weissenborn, Xiaohua Zhai, Thomas Unterthiner, Mostafa Dehghani, Matthias Minderer, Georg Heigold, Sylvain Gelly, Jakob Uszkoreit, and Neil Houlsby. An image is worth 16x16 words: Transformers for image recognition at scale. In *International Conference on Learning Representations*, 2021.
- Emilien Dupont, Hyunjik Kim, SM Ali Eslami, Danilo Jimenez Rezende, and Dan Rosenbaum. From data to functa: Your data point is a function and you can treat it like one. In *International Conference on Machine Learning*, 2022a.
- Emilien Dupont, Yee Whye Teh, and Arnaud Doucet. Generative models as distributions of functions. In *International Conference on Artificial Intelligence and Statistics*, 2022b.
- Arthur Gretton, Olivier Bousquet, Alex Smola, and Bernhard Schölkopf. Measuring statistical dependence with hilbert-schmidt norms. In *International conference on algorithmic learning theory*, 2005.
- Richard W Hamming. Error detecting and error correcting codes. *The Bell system technical journal*, 29(2):147–160, 1950.
- Kaiming He, Xiangyu Zhang, Shaoqing Ren, and Jian Sun. Deep residual learning for image recognition. In *Proceedings of the IEEE conference on computer vision and pattern recognition*, 2016.
- Minyoung Huh, Brian Cheung, Tongzhou Wang, and Phillip Isola. Position: The platonic representation hypothesis. In *International Conference on Machine Learning*, 2024.
- Ioannis Kalogeropoulos, Giorgos Bouritsas, and Yannis Panagakis. Scale equivariant graph metanetworks. In *Advances in neural information processing systems*, 2024.
- Miltiadis Kofinas, Boris Knyazev, Yan Zhang, Yunlu Chen, Gertjan J. Burghouts, Efstratios Gavves, Cees G. M. Snoek, and David W. Zhang. Graph neural networks for learning equivariant representations of neural networks. In *International Conference on Learning Representations*, 2024.
- Simon Kornblith, Mohammad Norouzi, Honglak Lee, and Geoffrey Hinton. Similarity of neural network representations revisited. In *International conference on machine learning*, 2019.
- Derek Lim, Haggai Maron, Marc T. Law, Jonathan Lorraine, and James Lucas. Graph metanetworks for processing diverse neural architectures. In *International Conference on Learning Representations*, 2024.
- Luca De Luigi, Adriano Cardace, Riccardo Spezialetti, Pierluigi Zama Ramirez, Samuele Salti, and Luigi di Stefano. Deep learning on implicit neural representations of shapes. In *International Conference on Learning Representations*, 2023.
- Mayug Maniparambil, Raiymbek Akshulakov, Yasser Abdelaziz Dahou Djilali, Mohamed El Amine Seddik, Sanath Narayan, Karttikeya Mangalam, and Noel E O’Connor. Do vision and language encoders represent the world similarly? In *Proceedings of the IEEE/CVF Conference on Computer Vision and Pattern Recognition*, 2024.
- Aviv Navon, Aviv Shamsian, Idan Achituve, Ethan Fetaya, Gal Chechik, and Haggai Maron. Equivariant architectures for learning in deep weight spaces. In *International Conference on Machine Learning*, 2023.
- Samuele Papa, Riccardo Valperga, David Knigge, Miltiadis Kofinas, Phillip Lippe, Jan-Jakob Sonke, and Efstratios Gavves. How to train neural field representations: A comprehensive study and benchmark. In *Proceedings of the IEEE/CVF Conference on Computer Vision and Pattern Recognition*, 2024.
- Maithra Raghu, Thomas Unterthiner, Simon Kornblith, Chiyuan Zhang, and Alexey Dosovitskiy. Do vision transformers see like convolutional neural networks? *Advances in neural information processing systems*, 2021.

Aviv Shamsian, Aviv Navon, David W Zhang, Yan Zhang, Ethan Fetaya, Gal Chechik, and Haggai Maron. Improved generalization of weight space networks via augmentations. In *International Conference on Machine Learning*, 2024.

Vincent Sitzmann, Julien Martel, Alexander Bergman, David Lindell, and Gordon Wetzstein. Implicit neural representations with periodic activation functions. *Advances in neural information processing systems*, 2020.

Thomas Unterthiner, Daniel Keysers, Sylvain Gelly, Olivier Bousquet, and Ilya Tolstikhin. Predicting neural network accuracy from weights. *arXiv preprint arXiv:2002.11448*, 2020.

Taesun Yeom, Sangyoon Lee, and Jaeho Lee. Fast training of sinusoidal neural fields via scaling initialization. In *International Conference on Learning Representations*, 2025.

Allan Zhou, Kaien Yang, Kaylee Burns, Adriano Cardace, Yiding Jiang, Samuel Sokota, J Zico Kolter, and Chelsea Finn. Permutation equivariant neural functionals. *Advances in neural information processing systems*, 2023.

APPENDIX

A RELATED WORK

Weight space learning and metanetworks. The study of weight space learning begins with the observation that statistics of neural network parameters contain information (*e.g.*, generalization properties of NN) (Unterthiner et al., 2020). The next approaches involve building neural methods for deep learning on weights for various downstream tasks, where these type of architectures are referred to as “metanetworks” or “neural functionals”. The major building blocks of metanetworks (MNs) involve designing architectures that account for the symmetries of weight space (*e.g.*, permutation, scaling, etc.). The early works in MNs consider applying permutation-equivariant layers (Navon et al., 2023; Zhou et al., 2023), based on blueprint of “geometric deep learning” (Bronstein et al., 2021). But these approaches are often not “versatile” since they cannot handle heterogeneous architectures in a dataset. More recent approaches focus on better representations of parameters. Lim et al. (2024) and Kofinas et al. (2024) suggest representing parameters as a “graph” and learning representations using graph neural networks, which is called as graph metanetworks (GMNs). Kalogeropoulos et al. (2024) improve GMNs by considering additional symmetries inherent in neural network weights, specifically scaling (or sign) symmetry. While these GMNs outperform prior works on various tasks, a major concern remains unaddressed: *GMNs still perform poorly compared to traditional data-based neural networks and why*. To fill this gap, it is crucial to understand GMNs and the difference between data-based and parameter-based learning. In line of this, we take a first step toward understanding GMNs, specifically from a representation perspective.

Implicit neural representations as data. Implicit neural representations (INRs) are a family of neural networks that map spatiotemporal coordinates to signal values, *e.g.*, image INRs learn a mapping from coordinates in a 2D Euclidean domain to RGB values. Since an INR represents a single datum, some recent works consider each INR as a datum itself—more precisely, its parameters as a datum. The paradigm of “INRs as data” offer the possibility of storing continuous signal in an efficient manner (Dupont et al., 2022b;a), which is totally different from traditional data representations. Luigi et al. (2023) uses an auto-encoding scheme to learn a latent space of INR functions solely from parameters, which are input as flattened vectors. Papa et al. (2024) studies the trade-off between the “reconstruction quality of INRs” and the “learnability from INR parameters.” Yeom et al. (2025) analyzes the effect of the initialization scheme (*i.e.*, variance of initialization distribution) of INRs on learning in weight space. Despite this line of work, it has been observed that state-of-the-art INR-processing networks (*i.e.*, Kalogeropoulos et al. (2024)) perform poorly on some tasks. For instance, CIFAR-10 INR classification achieves only about 37%, compared to CIFAR-10 image classification on traditional neural networks, which reaches nearly 99%, while the reasons remain unknown. In this work, we study the phenomena arising in INR classification (using GMNs) versus image classification (using MLPs and CNNs), specifically in terms of their internal representations.

Internal representations of neural networks. As part of efforts to understand NNs, interest in their internal representations has persisted over time. Kornblith et al. (2019) study the activation matrices of CNNs and reveal that differently initialized CNNs learn similar features. Raghu et al. (2021) comprehensively evaluate the representations between CNNs (*e.g.*, ResNets (He et al., 2016)) and Vision Transformers (ViTs) (Dosovitskiy et al., 2021), finding correspondences between blocks or layers. Maniparambil et al. (2024) reveal that text encoders and image encoders share representations, as indicated by higher CKA values, a similar observation also noted in Huh et al. (2024). In the field of metanetworks, Shamsian et al. (2024) study data augmentation in weight space to improve generalization of metanetworks.

	GMN (INR input)	MLP (image input)	CNN (image input)
MNIST	95.92 ± 0.31 [50, 1e - 03]	96.13 ± 0.24 → 98.74 ± 0.11 [10, 1e - 04] → [20, 1e - 04]	96.06 ± 0.27 → 98.31 ± 0.11 [5, 5e - 05] → [20, 5e - 05]
Fashion-MNIST	77.83 ± 0.63 [30, 1e - 03]	78.19 ± 0.42 [20, 1e - 05]	79.60 ± 0.41 [20, 1e - 05]
CIFAR-10	35.73 ± 1.23 [100, 1e - 03]	36.91 ± 0.45 [25, 1e - 05]	38.02 ± 0.36 [10, 1e - 05]

Table 2. **Test accuracies (%) across datasets and tasks & hyperparameters.** Values in [square brackets] represent [training epochs, learning rate], respectively. We additionally report details of more intense training in Section 3.1 and Section 3.3 as blue.

B EXPERIMENTAL DETAILS

B.1 DATASET DETAILS

We consider three different datasets for experiments, details are as follows.

- **MNIST:** We use MNIST image dataset for general NNs, and MNIST INR dataset from Navon et al. (2023). Each dataset contains 55k training images/INRs, 5k validation images/INRs, and 10k test images/INRs.
- **Fashion-MNIST:** We use Fashion-MNIST image dataset for general NNs, and Fashion-MNIST INR dataset also from Navon et al. (2023). Each dataset contains 55k training images/INRs, 5k validation images/INRs, and 10k test images/INRs.
- **CIFAR-10:** We use CIFAR-10 image dataset for general NNs, and CIFAR-10 INR dataset from Zhou et al. (2023). Each dataset contains 45k training images/INRs, 5k validation images/INRs, and 10k test images/INRs.

For all experiments, we report “test accuracy,” where all test datasets are class-balanced. For INRs, we use three-layer SIREN (Sitzmann et al., 2020), with 32 as a hidden dimension.

B.2 NETWORK DETAILS

- **GMN:** We adopt ScaleGMN (Kalogeropoulos et al., 2024) for a architecture of GMN. Specifically, we use default setup of ScaleGMN without bidirectional message passing. Precisely, each node (*i.e.*, bias) and directed edge (*i.e.*, weight) of the neural graph are projected into a higher dimensional feature space via linear networks and trained using a message passing algorithm designed to account for the sign symmetries in SIREN INR (Section 5 in Kalogeropoulos et al. (2024)). Aggregation occurs at the output nodes of neural graphs after four steps of message passing. Here, we refer to “the updated features of output node(s) after k steps” as “ k -th hidden representations,” which share a similar concept with activation matrices in general NNs.
- **MLP:** We use simple four-hidden layer MLP architecture, with 128 (for MNIST and Fashion-MNIST) or 192 (for CIFAR-10) hidden dimension with ReLU activation functions.
- **CNN:** In this case, we also use a simple four-hidden layer CNN architecture. Convolutional layers consist with (1) 128 (for MNIST and Fashion-MNIST) or 192 (for CIFAR-10) 7×7 filters with stride 3 and (2,3,4) 128 (for MNIST and Fashion-MNIST) or 192 (for CIFAR-10) 2×2 filters with stride 2. Since the activation matrices of CNNs have multiple channels, we apply average pooling if the number of channels is greater than one.

B.3 ADDITIONAL DETAILS

We train each networks for ten different seeds with AdamW optimizer. Additionally, for fair comparison between representations, we trained general neural networks until they reached the best test accuracy of GMNs for each task. We report test accuracies, training epochs, and learning rates in Table 2.

C ADDITIONAL RESULTS

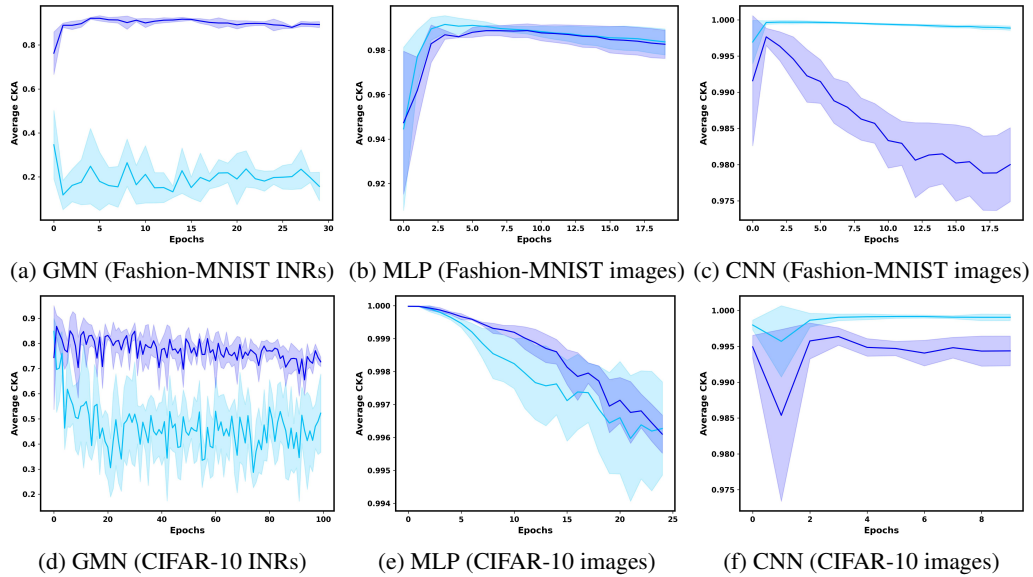


Figure 3. **Averaged CKA over five pairs of random GMNs, MLPs, and CNNs in Fashion-MNIST and CIFAR-10 classification.** The skyblue plot represents the averaged CKA(3, a), while the blue plot represents the averaged CKA(4, a) for each architecture. Note that the range of CKA varies significantly across datasets.

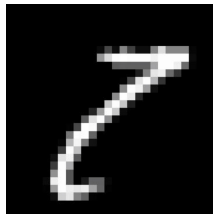


Figure 4. **Sample analysis.** A sample in which the prediction of general NNs is always incorrect, while that of GMNs is always correct, across different initialization.